

The IRAS cirrus and the diffuse ultraviolet background

P. Jakobsen, J. S. de Vries*, and F. Paresce**

Astrophysics Division, Space Science Department of ESA, ESTEC, 2200 AG Noordwijk, The Netherlands

Received December 1, 1986; accepted March 19, 1987

Summary. We show that a correlation exists at high and intermediate galactic latitudes between the diffuse infrared background intensity at $100\ \mu\text{m}$ as measured by IRAS and the diffuse background intensity in the far ultraviolet. The slope of this correlation is in reasonable quantitative agreement with the expected ratio between scattered and thermal emission from high latitude low albedo dust grains illuminated and heated by the integrated interstellar radiation field. The existence of this correlation thus provides strong observational support for both the dust back-scattering explanation for the known correlation between diffuse UV background and line-of-sight 21 cm column density, and the closely related radiatively heated grain emission model for the IRAS cirrus phenomenon.

Key words: cosmic background radiation – infrared radiation – UV radiation – interstellar medium: dust

1. Introduction

The cosmic background radiation at both infrared and ultraviolet wavelengths carries unique information concerning a wide variety of topics, ranging from the properties of interstellar grains to the existence of intergalactic matter and exotic massive particles (cf. Stecker et al., 1977; Paresce and Jakobsen, 1980). It is therefore of considerable interest to be able to separate the various contributions to the integrated diffuse emission seen at these wavelengths.

An important clue as to the origin of at least part of the diffuse ultraviolet background observed at high and intermediate galactic latitudes, can be found in the positive correlation between background intensity and line of sight neutral hydrogen column density first pointed out by Paresce et al. (1980) and later confirmed by a number of other experiments (Joubert et al., 1983; Zvereva et al., 1982; and Jakobsen et al., 1984). The existence of this correlation is generally accepted as evidence for a substantial galactic component to the ultraviolet background due to galactic plane starlight scattered off high latitude interstellar dust mixed in with the neutral hydrogen (Jura 1979; Jakobsen 1982).

Send offprint requests to: P. Jakobsen

* Presently at the Physics and Electronics Laboratory of TNO, The Hague

** Assigned to the Space Telescope Science Institute

More recently, the Infrared Astronomical Satellite (IRAS) mission has confirmed that a similar situation exists in the far-infrared, in that the diffuse emission at high and intermediate galactic latitudes in the IRAS $60\ \mu\text{m}$ and $100\ \mu\text{m}$ bands includes a patchy 'cirrus' component that also correlates with neutral hydrogen column density (Low et al., 1984; Boulanger et al., 1985; de Vries and Le Poole, 1985). The origin of the IRAS cirrus is believed to be thermal radiation from high latitude dust grains heated by the ambient interstellar radiation field (Stecker et al., 1977; Mezger et al., 1982).

If these interpretations are correct, then the interstellar dust contributions to the background at ultraviolet and infrared energies should clearly be intimately related, with the ultraviolet background sampling the back-scattered component of the illuminating radiation and the infrared background the truly absorbed component. Furthermore, if radiative scattering and absorption followed by thermal re-emission are, in fact, the dominant processes involved, then the ratio of the intensities of the background at ultraviolet and infrared energies should be independent of the gas-to-dust ratio, and mainly depend on the albedo of the grains and the relative spectral shape of the incident radiation field. Thus the availability of the IRAS sky maps provides a unique opportunity to correlate the ultraviolet data with the dust directly, and test the theory for the origin of the cirrus in the process.

In this paper we present the results of a first comparison between the ultraviolet background data of Jakobsen et al. (1984) and the IRAS $100\ \mu\text{m}$ *Spline 1* maps. In Sect. 2 we demonstrate that the anticipated correlation between diffuse emission in the ultraviolet and infrared is present in the data, and in Sect. 3 we argue that the slope of the correlation is in reasonable quantitative agreement with that theoretically expected, given our present knowledge of the detailed radiative properties of interstellar grains.

2. The observed UV versus IR correlation

For the purpose of this investigation, we have focused on the subset of the ultraviolet sounding rocket data of Jakobsen et al. (1984) that pertains to a $50^{\circ}.5$ scan carried out at an intermediate galactic latitude of $b \simeq 50^{\circ}$. These data were obtained with three broad-band photometers having 0.5° diameter fields of view, and consist of absolute background intensity measurements for 79 targets at the effective wavelengths $2135\ \text{\AA}$, $1710\ \text{\AA}$, and $1590\ \text{\AA}$, respectively (see Jakobsen et al., 1984 for details). For each of

these 79 fields, the corresponding mean IRAS 100 μm and 60 μm infrared fluxes were obtained from the Groningen IRAS *Spline 1* maps by averaging over the relevant UV target areas. The in-band *Spline 1* fluxes were converted to specific intensity in units of $\text{ergs s}^{-1} \text{cm}^{-2} \text{\AA}^{-1} \text{sr}^{-1}$ by adopting effective bandwidths of 33 μm and 31 μm for the 100 μm and 60 μm bands, respectively. The flux-scale correction factors of 0.75 and 0.68 for the *Spline 1* fluxes quoted by Laureijs (1985) were also applied to the data.

Based on the work of Jongeneelen et al. (1986), we estimate that at the ecliptic latitudes of the targets ($40^\circ \leq \beta \leq 64^\circ$), the zodiacal infrared emission contribution to the IRAS intensities is $\leq 20\%$ at 60 μm , and for practical purposes negligible at 100 μm . As discussed in Jakobsen et al. (1984), a similar situation

holds for the ultraviolet data, in that the two short wavelength datasets are entirely free of zodiacal emission, whereas the 2135 \AA fluxes probably contain a zodiacal emission component at the $\approx 30\%$ level. The 2135 \AA intensities were also subject to a substantial correction for nitric oxide airglow emission. In view of these complications, we will in the following primarily focus on correlating the longest wavelength, 100 μm infrared intensities with the shortest wavelength, 1710 \AA ultraviolet intensities.

Fig. 1 shows the run of the IRAS 100 μm intensity along the scan path, together with the corresponding 21 cm hydrogen column densities and representative 1710 \AA ultraviolet intensities, also in units of $\text{ergs s}^{-1} \text{cm}^{-2} \text{\AA}^{-1} \text{sr}^{-1}$. Figures 2 and 3 show

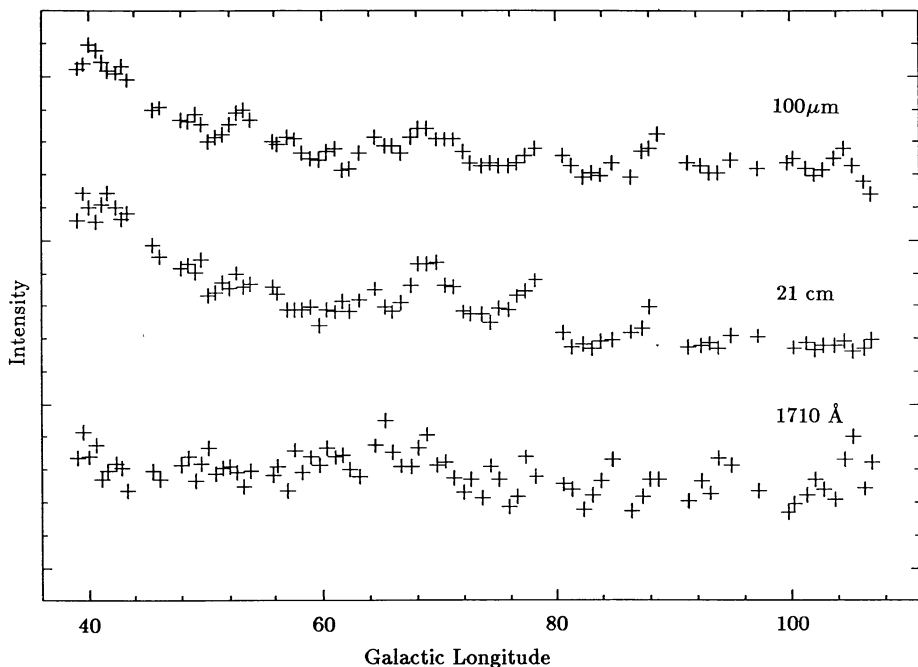


Fig. 1. Run of the IRAS 100 μm intensity (upper frame), 21 cm hydrogen column density (center frame), and 1710 \AA ultraviolet intensity (lower frame), along the region scanned

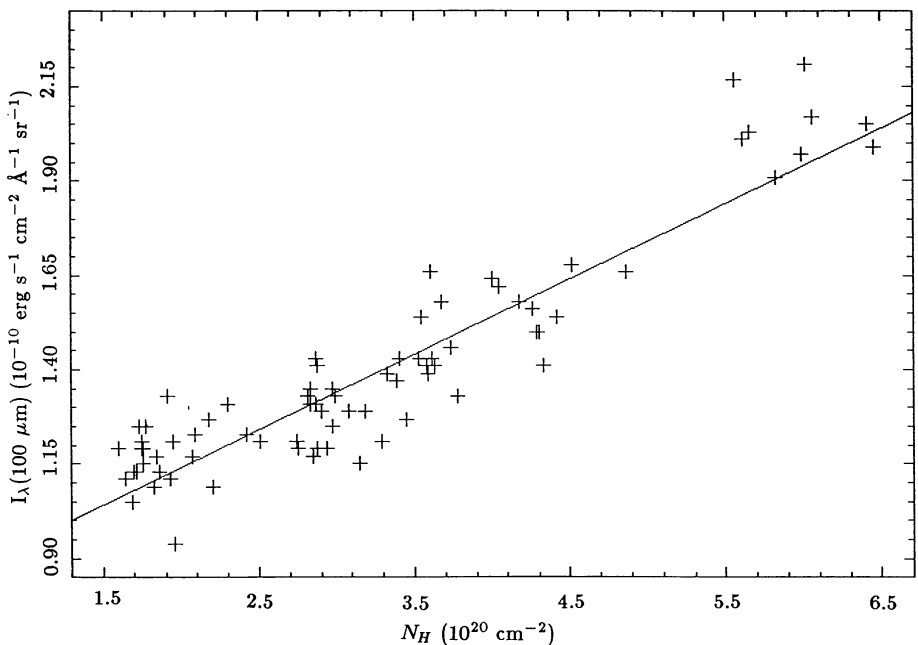


Fig. 2. Correlation between the 100 μm infrared intensities and 21 cm column densities displayed in Fig. 1

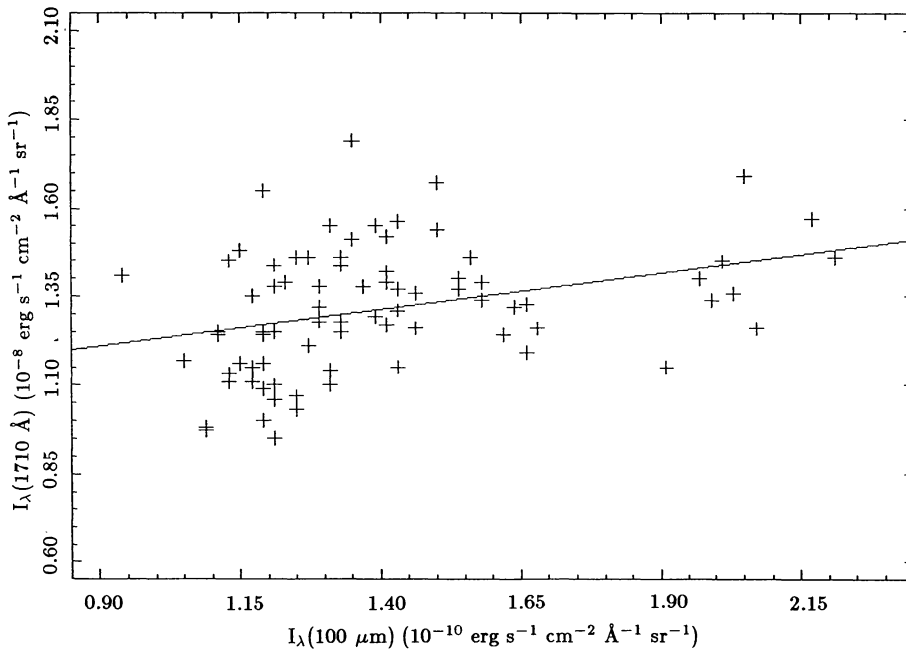


Fig. 3. Correlation between the 1710 Å ultraviolet intensities and 100 μm infrared intensities displayed in Fig. 1

the corresponding correlation plots between the infrared data and the 21 cm and ultraviolet 1710 Å data, respectively. As is clear from these figures, the IRAS 100 μm intensity shows a good correlation with line of sight 21 cm column density ($\rho = 0.926$). We note that the slope and zero-column offset of this correlation correspond to, respectively, $(58 \pm 26) \times E(B - V) \text{ MJy sr}^{-1} \text{ mag}^{-1}$ and $(0.39 \pm 0.2) \text{ MJy sr}^{-1}$, values in close agreement with those quoted by Rowan-Robinson (1986). The positive correlation with the 1710 Å ultraviolet background intensity, although nowhere as striking, is still significant at the 3σ confidence level because of the large number of points involved in the analysis ($\rho = 0.329$, 79 data points). The infrared versus ultraviolet correlation plots for the 2135 Å and 1590 Å data displayed in Figs. 4 and 5 are

similar in appearance to that of the 1710 Å data, although they display respectively stronger and weaker correlations. Table 1 also lists the statistics of the correlations for the data at these wavelengths.

As discussed in detail by Jakobsen et al. (1984) the ultraviolet data described above display significant correlations with line of sight neutral hydrogen density. Hence, in view of the good correlation between IRAS 100 μm intensity and N_{H} exhibited in Fig. 1, one should not be surprised to find a similar correlation between the UV and IR fluxes.

It is interesting to note, however, that the UV versus IR correlations of Table 1 are no better, and actually considerably more noisy than the UV versus 21 cm correlations shown in Jakobsen

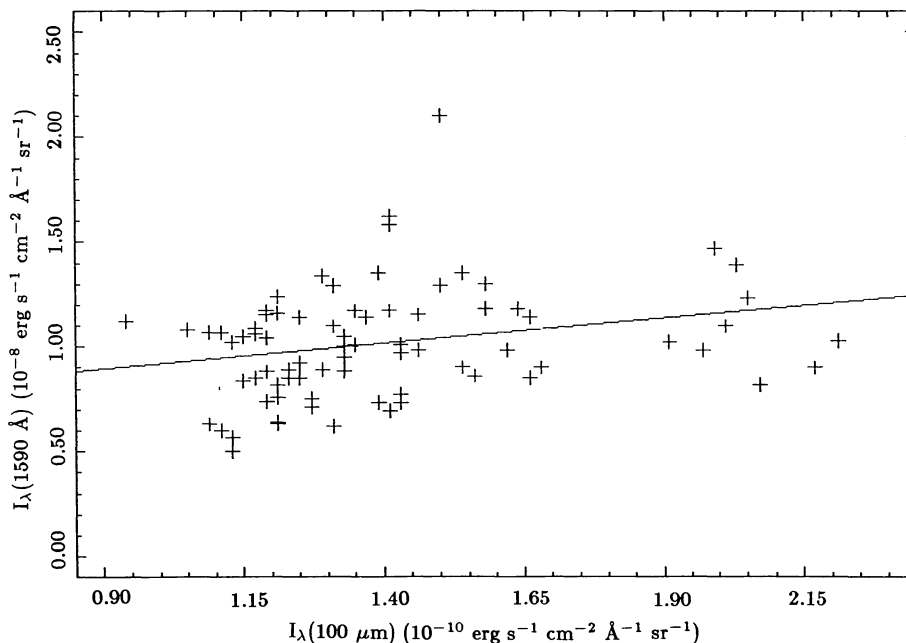


Fig. 4. Correlation between the 1590 Å ultraviolet intensities and 100 μm infrared intensities

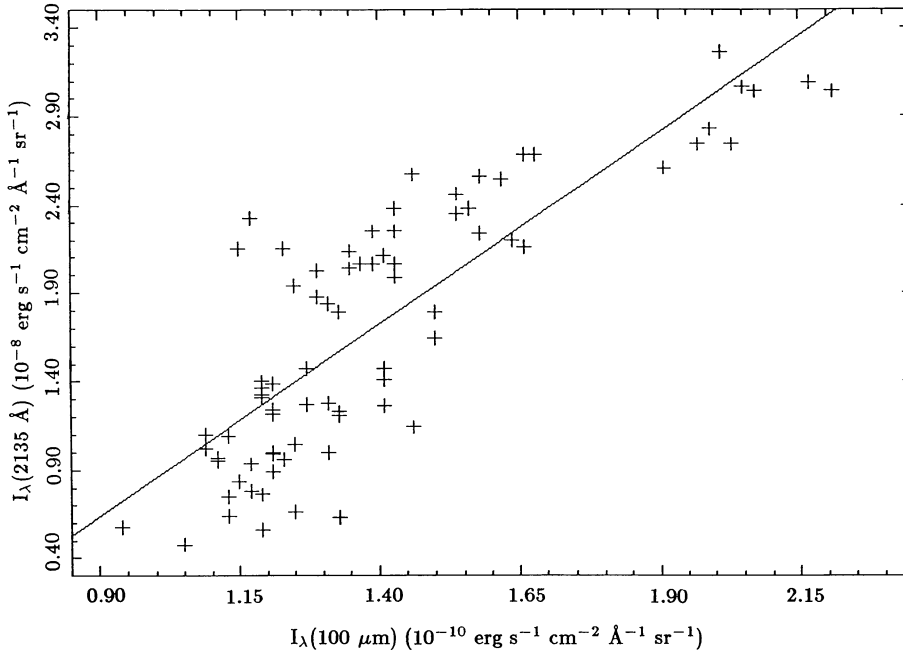


Fig. 5. Correlation between the 2135 Å ultraviolet intensities and 100 μm infrared intensities

Table 1. 100 μm IR versus UV intensity correlations

Wavelength (Å)	ρ^a	Observed slope ^b	Predicted ratio ^b
1590	0.253	$(2.4 \pm 1.0) 10^1$	$9.9 10^1$
1710	0.329	$(2.1 \pm 0.7) 10^1$	$9.6 10^1$
2135	0.827	$(2.2 \pm 0.2) 10^2$	$1.0 10^2$

^a Rank correlation coefficient, 79 data points

^b Monochromatic UV-to-IR intensity ratio in units of $\text{ergs s}^{-1} \text{cm}^{-2} \text{Å}^{-1} \text{sr}^{-1}$

et al. (1984). However, the IRAS *Spline 1* maps suffer from a strong amount of residual “streakiness” due to calibration drift between scans. This, combined with the $\approx 15\%$ relative photometric accuracy of the UV intensities, is sufficient to explain the scatter around the trend of the data.

The parameter of interest for this investigation is the average ratio between back-scattered ultraviolet intensity and re-emitted infrared intensity. We have determined this average ratio from the slopes of the standard least-squares linear regression fits to the data. The third column in Table 1 lists the values of the dimensionless ratio $\langle I_\lambda(\text{UV})/I_\lambda(100\mu) \rangle$ determined in this manner, along with the formal statistical errors. Note that the approach of including a constant term in the regression fit in principle allows for potential baseline calibration errors in both data sets, as well as the possible existence of isotropic (i.e. local and/or extragalactic) components to the backgrounds in the ultraviolet and infrared. As for the absolute uncertainty in the derived values of $\langle I_\lambda(\text{UV})/I_\lambda(100\mu) \rangle$, the absolute calibrations of both the ultraviolet and infrared data certainly should be good to within a factor of two, and therefore, their ratio ought to be accurate to within a factor of three or better. This overall error budget is probably not unreasonable in light of the fact that the derived UV to IR diffuse intensity ratios combine absolute

flux measurements from two unrelated space experiments separated by more than two orders of magnitude in photon energy.

3. Interpretation

Consider a diffuse interstellar cloud at high galactic latitude having dust optical depth, τ_λ , in the ultraviolet. Since the O and B stars responsible for the bulk of the UV radiation in the Galaxy are confined to the galactic plane, the cloud will to a first approximation be illuminated by UV starlight of roughly constant intensity, I_λ^* , within the hemisphere facing the Galaxy. In the optically thin ($\tau_\lambda \leq 1$) limit the back-scattered UV intensity will therefore be given by (Jura, 1979)

$$I_\lambda(\text{UV}) \simeq \frac{1}{2} a_\lambda H(g_\lambda, b) I_\lambda^* \tau_\lambda, \quad (1)$$

where a_λ is the grain albedo, and $0 \leq H(g, b) \leq 1$ is an appropriate integral over the Henyey-Greenstein phase function that depends on the scattering asymmetry parameter of the grains, g_λ , and the galactic latitude, b , of the cloud. If the gas-to-dust ratio is represented by the usual ratio $[N_{\text{H}}/E(B-V)]$, the relationship between dust optical depth and line-of-sight neutral hydrogen column density is

$$\tau_\lambda = 0.921 \frac{R_\lambda}{[N_{\text{H}}/E(B-V)]} N_{\text{H}}, \quad (2)$$

where $R_\lambda = A_\lambda/E(B-V)$ is the normalized extinction at wavelength λ . As discussed in more detail in Jakobsen (1982) and Jakobsen et al. (1984), the quantitative agreement between the slope of the observed UV intensity versus N_{H} correlation and that predicted by Eqs. (1) and (2) is as good as one could hope for, given our knowledge of the various parameters entering the problem. The data are consistent with the high latitude interstellar material having a normal gas-to-dust ratio, and moderately forward-scattering grains having far-UV scattering parameters

$a_\lambda \simeq 0.4$ and $g \simeq 0.6$ as predicted by the more sophisticated models for interstellar grains available. For these parameters, typical diffuse clouds having $N_H \simeq 10^{20} - 10^{21} \text{ cm}^{-2}$ will back-scatter at levels of 1–10% of the incident stellar flux. A comparable amount of radiation will be truly absorbed by the dust and lead to heating of the grains. In the notation introduced above, the intensity of the resulting thermal emission can be expressed as

$$I_\lambda(\text{IR}) \simeq \frac{1}{2} \left[\int_0^\infty (1 - a_\lambda) \tau_\lambda I_\lambda^* d\lambda \right] \frac{d\phi}{d\lambda}, \quad (3)$$

where the integral in brackets is proportional to the total amount of incident radiation absorbed at all wavelengths by the grains along the line of sight, and $d\phi/d\lambda$ denotes the normalized spectrum of the thermal emission. For grains absorbing as $\sigma_\lambda \propto \lambda^{-n}$ in the infrared, we have from Kirchoff's Law

$$\frac{d\phi}{d\lambda}(T) \simeq \left(\frac{1}{\lambda} \right) \frac{(hc/kT\lambda)^{4+n}}{(e^{hc/kT\lambda} - 1) \Gamma(4+n) \zeta(4+n)}. \quad (4)$$

From these expressions it follows that the anticipated ratio between back-scattered UV intensity and re-emitted thermal IR intensity can be written

$$\frac{I_\lambda(\text{UV})}{I_\lambda(\text{IR})} \simeq \frac{a_\lambda H(g_\lambda, b) R_\lambda I_\lambda^*}{\left[\int_0^\infty (1 - a_\lambda) R_\lambda I_\lambda^* d\lambda \right] \frac{d\phi}{d\lambda}(T)}. \quad (5)$$

Note that Eq. (5) is independent of both N_H and the gas-to-dust ratio, and only depends explicitly on the spectral shape of the incident radiation field and grain absorption and scattering cross-sections. The absolute intensity of the incident radiation field and the physical grain size do enter implicitly, however, through the steady-state grain temperature appearing in $d\phi/d\lambda$.

In evaluating Eq. (5) we have, following Jakobsen et al. (1984), adopted the average total extinction curve given by Savage and Mathis (1979), and the scattering parameters calculated by White (1979) for the Mathis et al. (1977) grain model. For the incident stellar radiation field, I_λ^* , we have adopted the intensities given by Gondhalekar et al. (1980), supplemented with the values compiled by Mezger et al. (1982) for wavelengths above 3000 Å. For these values we obtain for the integrated grain absorption rate: $4\pi \left[\int_0^\infty (1 - a_\lambda) R_\lambda I_\lambda^* d\lambda \right] \simeq 2.4 \cdot 10^{-2} \text{ ergs s}^{-1} \text{ cm}^{-2}$. With a canonical gas-to-dust ratio of $N_H/E(B - V) \simeq 5.8 \cdot 10^{21} \text{ cm}^{-2} \text{ mag}^{-1}$ (Bohlin et al., 1978), this is equivalent to an absorption rate of $3.8 \cdot 10^{-24} \text{ ergs s}^{-1}$ per hydrogen atom, in good agreement with the value of $4.2 \cdot 10^{-24} \text{ ergs s}^{-1}$ derived by Mezger et al. (1982). It is interesting to point out that because of the rapid rise in the interstellar radiation density at wavelengths above $\approx 3000 \text{ Å}$ caused by the abundance of cooler stars in the Galaxy, a substantial fraction of the radiative absorption actually takes place in the visible and near-infrared region of the spectrum. About 20% of the total absorption occurs in the 1450–2500 Å segment of the spectrum spanned by the ultraviolet data at hand, which is comparable to that absorbed in the *U*, *B* and *V* bandpasses in the visible.

Given complete knowledge of the detailed grain properties, it is in principle possible to predict the steady-state grain temperature for any value of the total bolometric radiative absorption rate. However, considerable complications arise if realistic variations in physical grain size and chemical composition are taken into account (cf. Mezger et al., 1982). We have therefore

determined the effective grain temperature empirically from the observed infrared color of the cirrus.

The 100 μm and 60 μm IRAS intensities along the region scanned display a very tight linear correlation ($\rho \simeq 0.95$) with a slope of $\langle I_\lambda(100\mu)/I_\lambda(60\mu) \rangle \simeq 0.52$. For an assumed $\sigma_\lambda \propto \lambda^{-1.5}$ absorption law, the color temperature of the dust corresponding to this ratio is 36 K, somewhat larger than the theoretical values of $T \simeq 10 \text{ K}$ for silicate grains and $T \simeq 19 \text{ K}$ for graphite grains predicted by Mezger et al. (1982). The parameter of interest in the present context, however, is not so much the physical grain temperature, but the relative monochromatic thermal emission at 100 μm . For $T \simeq 36 \text{ K}$ and $n = 1.5$, we obtain from Eq. (4): $d\phi/d\lambda \simeq 7.1 \cdot 10^{-7} \text{ Å}^{-1}$. We note that although the precise value of the derived grain color temperature is rather sensitive to the assumed infrared absorption law (and any residual zodiacal emission contamination in the 60 μm bandpass), the parameter $d\phi/d\lambda$ is actually remarkably robust in that its value varies by less than 50% for any realistic combination of grain temperature in the range $T \simeq 20 - 40 \text{ K}$ and absorption law index $n \simeq 1 - 2$. The reason for this behavior is that the observed infrared color of the cirrus places the 100 μm bandpass near the peak of the modified Planck curve. Hence, despite of our slightly inconsistent method of establishing the effective grain temperature, our adopted predicted value of the parameter $d\phi/d\lambda$ is in all likelihood reasonably well-determined. The last column of Table 1 lists the resulting theoretical ultraviolet to 100 μm infrared intensity ratios predicted by Eq. (5).

4. Discussion

From Table 1 it can be seen that the anticipated diffuse UV to 100 μm IR intensity ratios derived above agree with the observed ratios to within a factor of four at 1710 Å and 1590 Å, and to within a factor of two at 2135 Å. We regard this level of agreement to be highly satisfactory, given the absolute accuracy of the observations and our level of knowledge of the detailed interstellar grain properties. Nonetheless, taken at face value, the discrepancy between theory and observations for the more reliable data at the shorter ultraviolet wavelengths is in the sense of the infrared cirrus being brighter than expected with respect to the back-scattered ultraviolet emission. If real, such a discrepancy could be explained in several ways.

Firstly, note that according to Eq. (5) the ultraviolet to infrared emission ratio scales with grain scattering parameters roughly as $I_\lambda(\text{UV})/I_\lambda(\text{IR}) \propto a_\lambda(1 - g_\lambda)/(1 - \langle a_\lambda \rangle)$. Hence if the actual grain albedo and asymmetry parameter differ from the values of $\langle a_\lambda \rangle \simeq 0.5$ and $g_\lambda \simeq 0.6$ predicted in the Mathis et al. (1977) grain model, then the resulting UV-to-IR ratio could be substantially lower than the values listed in Table 1. We note that grain models having the required combination of low a_λ and high g_λ have recently been proposed by Chlewicki and Greenberg (1984).

A second possibility is that the high latitude dust clouds are not completely optically thin as assumed in the derivation of Eq. (5). In fact, the range of N_H sampled by the observations implies for a normal gas-to-dust ratio and extinction curve rather high line-of-sight optical depths of the order $\tau_\lambda \simeq 0.2 - 1.2$ in the far-ultraviolet, which may strain the validity of our simple model. It is extremely difficult to quantify the deviations from Eq. (5) expected due to multiple scattering and optical depth effects, but the sense of the effect will clearly be to lower the amount of scattered radiation with respect to that truly absorbed, thereby

lowering the UV-to-IR emission ratio. Depending on the grain parameters and large scale geometry adopted, the magnitude of this effect could be quite substantial.

Yet another possibility is that the fluxes in the IRAS 60 μm and 100 μm bandpasses contain an additional contribution from collisionally excited [O I], [O II] and [C II] fine structure line radiation, as suggested recently by Harwit et al. (1986). However, the tight correlation between the cirrus intensity and N_{H} displayed in Fig. 2 would seem to rule out a major contribution from this source.

Finally, there are two potential additional processes that should work in the opposite sense of increasing the apparent ultraviolet to 100 μm infrared ratio. These are excess emission in the far ultraviolet caused by fluorescence in the Lyman and Werner bands of the H_2 molecule (Duley and Williams, 1980), and a reduction in the 100 μm output due to an excess of infrared emission at short wavelengths from a population of very small transiently heated interstellar grains (Boulanger et al., 1985). However, the effects caused by these last two processes are most likely much less than a factor of two in magnitude (Jakobsen et al., 1984; Puget et al., 1985).

In any case, and regardless of the uncertainties introduced by these potential complications, the outcome of this first comparison between diffuse ultraviolet and far infrared background intensities has provided strong observational support for both the dust back-scattering model for the known correlation between UV background intensity and 21 cm column density and the closely related radiatively heated grain emission model for the IRAS cirrus phenomenon.

References

- Bohlin, R.C., Savage, B.D., Drake, J.F.: 1978, *Astrophys. J.* **224**, 132
- Boulanger, F., Baud, B., van Albada, G.D.: 1985, *Astron. Astrophys.* **144**, L9
- Chlewicki, G., Greenberg, J.M.: 1984, *Monthly Notices Roy. Astron. Soc.* **211**, 719
- Duley, W.W., Williams, D.A.: 1980, *Astrophys. J. Letters* **242**, L179
- Gondhalekar, P.M., Phillips, A.P., Wilson, R.: 1980, *Astron. Astrophys.* **85**, 272
- Harwit, M., Houck, J.R., Stacey, G.J.: 1986, *Nature* **319**, 646
- Jakobsen, P.: 1982, *Astron. Astrophys.* **106**, 375
- Jakobsen, P., Bowyer, S., Kimble, R., Jelinsky, P., Grewing, M., Krämer, G., Wulf-Mathies, C.: 1984, *Astron. Astrophys.* **139**, 481
- Jongeneelen, A.A.W., Deul, E.R., Burton, W.B. 1986, *Astron. Astrophys.* (submitted)
- Joubert, M., Masnou, J.L., Lequeux, J., Deharveng, J.M., Cruvellier, P.: 1983, *Astron. Astrophys.* **128**, 114
- Jura, M.: 1979, *Astrophys. J.* **227**, 798
- Laureijs, R.: 1985, *Stuff 'n' nonsense – IRAS Newsletter* **3**, 7
- Low, F.J. et al.: 1984, *Astrophys. J. (Letters)* **278**, L19
- Mathis, J.S., Rumpl, W., Nordsieck, K.H.: 1977, *Astrophys. J.* **217**, 425
- Mezger, P.G., Mathis, J.S., Panagia, N.: 1982, *Astron. Astrophys.* **105**, 372
- Paresce, F., Jakobsen, P.: 1980, *Nature* **288**, 119
- Paresce, F., McKee, C.F., Bowyer, S. 1980, *Astrophys. J.* **240**, 387
- Puget, J.L., Lèger, A., Boulanger, F.: 1985, *Astron. Astrophys.* **142**, L19
- Rowan-Robinson, M.: 1986, in *Light on Dark Matter*, ed. Israel, F.P., D. Reidel, Dordrecht
- Savage, B.D., Mathis, J.S.: 1979, *Ann. Rev. Astron. Astrophys.* **17**, 73
- Stecker, F.W., Puget, J.L., Fazio, G.G.: 1977, *Astrophys. J. Letters* **214**, L51
- de Vries, C.P., Le Poole, R.S.: 1985, *Astron. Astrophys.* **145**, L7
- White, R.L.: 1979, *Astrophys. J.* **229**, 954
- Zvereva, A.M., Severny, A.B., Granitsky, L.V., Hua, C.T., Cruvellier, P., Courtes, G.: 1982, *Astron. Astrophys.* **116**, 312